The Isothermal Curing of a Diepoxide-cycloaliphatic Diamine Resin by Temperature Modulated Differential Scanning Calorimetry

S. MONTSERRAT, J. G. MARTÍN

Departament de Màquines i Motors Tèrmics, Universitat Politècnica de Catalunya, Carrer de Colom 11, E-08222-Terrassa, Spain

Received 1 August 2001; accepted 16 November 2001

ABSTRACT: The thermal properties and the isothermal cure of an epoxy resin based on diglycidyl ether of bisphenol A (DGEBA) with a diamine based on 4,4′-diamino-3,3′-dimethyldicyclohexylmethane (3DCM) were analyzed by differential scanning calorimetry (DSC) and temperature modulated DSC (TMDSC). The quasi-isothermal TMDSC scans were performed at curing temperatures between 40 and 140°C for different periods of time, and the modulation conditions were amplitude of 0.5K and a period of 60 s. The heating rates used on the DSC scans were between 2.5 and 20 $Kmin^{-1}$. The heat of curing measured nonisothermally increases when the heating rate decreases. An average value of 440 Jg^{-1} was estimated. The glass transition of the unreacted system measured by DSC was −40.4°C. The final glass transition temperature of the resin depends on the heating rate of cure and postcure conditions. Values between 143°C (measured by DSC) and 154°C (measured on the total heat flow by TMDSC) were obtained after isothermal curing and postcure at 10 and 1 $Kmin^{-1}$, respectively. The vitrification was analyzed by the modulus of the complex heat capacity $|C_p^*|$, which decay gives the interval and the time of vitrification. These properties were used to build the time–temperature–transformation cure diagram. The intensity of the vitrification was measured by the change in $|C_p^*|$, which decreases quasi-linearly with the curing temperature. The phase angle of the heat flow shows a peak in the vitrification region, which agrees with the vitrification time determined by $|C_p^*|$. The chemical kinetics may be fitted to a simplified autocatalytic model [$f(\alpha) = \alpha^m(1 - \alpha)^n$, Sesták-Berggren model] with an apparent activation energy of 58 $kJmol^{-1}$. The analysis of the diffusion controlled step is studied using a mobility factor determined from the normalised variation of $|C_p^*|$ during the vitrification. The simulated overall reaction rate, which is obtained from the product of the chemical kinetics and the mobility factor, agrees with the experimental reaction rate. © 2002 Wiley Periodicals, Inc. J Appl Polym Sci 85: 1263–1276, 2002

Key words: temperature modulated DSC (TMDSC); crosslinking; vitrification; thermosets

INTRODUCTION

Since the pioneering work of Fava[1] in 1968, differential scanning calorimetry (DSC) has been one of the most frequently used analytical techniques for studying the kinetics of the curing reaction of thermosetting polymers,[2] and especially of epoxy resins.[3,4] As is well known, the crosslinking reaction in an epoxy resin takes place in a condensed phase and, at the beginning, the kinetics is controlled by the chemical reaction of the functional groups. As the viscosity of the medium increases, the kinetics becomes controlled by the diffusion of the reactants, the degree of conver-

Correspondence to: S. Montserrat (montserrat@mmt.upc.es).

Contract grant sponsor: CICYT; contract grant number: MAT97-0634-C02-02.

Journal of Applied Polymer Science, Vol. 85, 1263–1276 (2002)

sion levels off and the system becomes a glass. The glass transition temperature (T_g) has been the property used in DSC to study this process of vitrification. As the degree of conversion increases due to the growing and crosslinking of the chains, the T_g of the system gradually increases. When this value becomes higher than the temperature of the system, the resin has reached the glassy state. The vitrification at a determined curing temperature, T_c, is studied in conventional DSC using the partial curing method, which allows both the T_g and the corresponding degree of conversion to be determined at different times. The vitrification time, t_v, is determined when T_g equals T_c.[2] These values determine the vitrification line in the time–temperature–transformation (TTT) cure diagram.[5]

Alternatively, other thermal analysis techniques such as dynamic mechanical analysis,[2,6] torsional braid analysis (TBA),[7,8] and dielectric relaxation spectroscopy (DRS)[9] have also been used to monitor the curing reaction and to study the relaxation associated with the vitrification phenomenon. In the nineties, Reading et al.[10,11] introduced the temperature-modulated differential scanning calorimetry (TMDSC), which has been shown to be a very useful technique for studying not only vitrification, but also the kinetics during the diffusion controlled step.[12–23]

In this work we study the thermal properties and the kinetic analysis of the isothermal cure of an epoxy resin based on diglycidyl ether of bisphenol A (DGEBA) with a diamine based on 4,4′-diamino-3,3′-dimethyldicyclohexylmethane (3DCM) in a stoichiometric ratio. The calorimetric techniques used in the work were conventional DSC and TMDSC. Complementary experiments of thermogravimetric analysis were performed to determine the limiting temperature to avoid thermal degradation. TMDSC was applied to study the vitrification process and to build the TTT diagram.

In 1990, Verchère et al.[24] studied the kinetics, the vitrification and the gelation of this system using conventional DSC and size-exclusion chromatography. Their precise results constitute an excellent reference for comparing and justifying the validity of our own, which was obtained by TMDSC. The interest in this epoxy–cycloaliphatic diamine resin lies in the increase of the pot life at room temperature.[24] This behavior is a consequence of the presence of the methyl group in a neighboring site to the amine group, which yields a steric hindrance that inhibits the reactivity of this amine group. This chemical structure produces a particular behavior in the curing kinetics and the vitrification of the system.

THE APPLICATION OF TMDSC TO CURING REACTION

The calorimetric measurement of a curing reaction by conventional DSC gives a unique heat flow signal, which includes the heat evolved during the curing and the so-called sensible heat due to the temperature dependence of the heat capacity of the sample. On the other hand, the measurements by TMDSC may give the heat of curing and the heat capacity of the system separately, apart from other properties.

As commented above, the kinetics of the curing reaction involves two different steps. Initially, the reaction is controlled by the chemical reactivity of the functional groups, and as the crosslinking progresses, the system vitrifies and the reaction becomes controlled by the diffusion of these groups through the medium. Both reactions are time dependent, showing different rates of reaction. According to the thermodynamics of irreversible processes,[25] a state function depends on temperature, pressure, and the variables ξ_i, which control the transformation. Therefore, the total enthalpy during the curing reaction in isobaric conditions is given by the following expression:

$$dH = \left(\frac{\partial H}{\partial T}\right)_{P,\xi_1,\xi_2} dT + \left(\frac{\partial H}{\partial \xi_1}\right)_{P,T,\xi_2} d\xi_1(t) + \left(\frac{\partial H}{\partial \xi_2}\right)_{P,T,\xi_1} d\xi_2(t) \quad (1)$$

where ξ_1 and ξ_2 are time-dependent variables, and

$$\left(\frac{\partial H}{\partial T}\right)_{P,\xi_1,\xi_2}$$

is the isobaric heat capacity that is temperature dependent and corresponds to the heat capacity defined in equilibrium thermodynamics. According to other authors[20,26] this heat capacity will be named static heat capacity, $C_{p,\mathrm{st}}(T)$. One of these variables, ξ_1, may be formally identified with the degree of conversion; the second term in eq. (1) then corresponds to the heat of reaction evolved during the chemical step, associated with the

variation of ξ_1 at T, P, and ξ_2 constants. The other variable, ξ_2, is identified with the extent of the reaction during the vitrification, and thus the third term corresponds to the enthalpy loss of the relaxation process. According to Schawe,[20] this third term may be related with a dynamic heat capacity, which is temperature and time dependent,

$$C_{p,dyn}(T,t) = \left(\frac{\partial H}{\partial \xi_2}\right)_{P,T,\xi_1} \frac{d\xi_2}{dT} \quad (2)$$

Taking into account these definitions and regrouping the terms, eq. (1) may be rewritten in the following form:

$$dH = \Delta H_r d\xi_1(t) + [C_{p,\mathrm{st}}(T) + C_{p,\mathrm{dyn}}(T,t)]dT \quad (3)$$

where ΔH_r is the heat of curing evolved for a sample of mass m. Accordingly, the heat flow ϕ may be derived from eq. (3) by dividing by dt:

$$\phi = \frac{dH}{dt} = \Delta H_r r + [C_{p,\mathrm{st}}(T) + C_{p,\mathrm{dyn}}(T,t)]q \quad (4)$$

where r is the reaction rate, $r = d\xi_1(t)/dt$, and q is the heating rate, $q = dT/dt$.

As TMDSC is based on the superimposition of a periodically varying temperature modulation upon the linear heating rate, the temperature as a function of time in the case of a sinusoidal modulation of amplitude A_T and frequency ω (radian s^{-1}) is given by the equation:

$$T = T_o + q_o t + A_T \sin(\omega t) \quad (5)$$

where T_o is the initial temperature and q_o is the underlying or average heating rate ($q_o = \Delta T/\Delta t$). Additionally, the periodic variation of the heating rate is given by the equation:

$$q = q_o + A_T \omega \cos(\omega t) \quad (6)$$

which in quasi-isothermal conditions is reduced to $q = A_T \omega \cos(\omega t)$.

As a consequence of the modulation of the heating rate, the heat flow also becomes modulated, as determined by eq. (4). Here, there is one part that corresponds to the heat of curing ($\Delta H_r\ r$), and another part that depends on the modulated heating rate q, corresponding to the periodic component of the heat flow.

The Fourier analysis of the cycles of the heating rate and the heat flow gives the following quantities:

1. The underlying or total heat flow $\langle\phi\rangle$, which in the isothermal curing is identified with the first summand of eq. (4) and gives the evolution of the heat flow during the curing. The total heat flow signal corresponds to the heat flow signal obtained by conventional DSC, and allows us to calculate the reaction rate $r = d\alpha/dt = \langle\phi\rangle/\Delta H_r$, where α is the degree of conversion. As usual, the degree of conversion at a determined time may be determined by the ratio of the partial heat of curing at this time, ΔH_t, and the total heat of curing ΔH_r.
2. According to the approach suggested by Schawe,[27] based on the linear response theory, a complex heat capacity may be defined as $C_p^* = C_p' - iC_p''$, where C_p' and C_p'' are, respectively, the real and imaginary parts of the heat capacity. The summand in brackets of eq. (4) is related to the real part of the complex heat capacity.[20,26] The modulus of the complex heat capacity is defined by the ratio of the heat flow amplitude, A_ϕ, and the heating rate amplitude, A_q ($A_q = A_T\ \omega$):

$$|C_p^*| = \frac{A_\phi}{A_q} \quad (7)$$

   The real and imaginary parts of the heat capacity are respectively defined by the following equations:

$$C_p' = |C_p^*| \cos\ \delta \quad (8)$$

$$C_p'' = |C_p^*| \sin\ \delta \quad (9)$$

   where δ is the phase angle, which is very small in the case of a relaxation process associated with the glass transition, as in the case of the vitrification. In these conditions, the values of $|C_p^*|$ and C_p' are practically indistinguishable, and the shape of C_p'' is very similar to that of the phase angle.
3. The phase angle δ measures the shift of the modulated heat flow signal with respect to the heating rate. The phase angle shows a peak when there is a relaxation process in the system, but this quantity is also influenced by the frequency, the change in the heat capacity of the sample, and the thermal conductance of the system composed by the sample-pan and the thermome-

ter.[28–30] In the case of the curing reaction, there is also the influence of the chemical reaction on δ.[20]

The main signals used in the present work are the total heat flow, which allows us to calculate the reaction rate and the degree of conversion, and the modulus of the complex heat capacity, which allows us to study the vitrification process and the kinetics during the step controlled by diffusion. The uncorrected phase angle will be used occasionally.

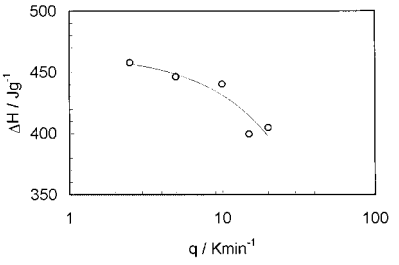

Figure 1 Variation of the heat of curing with the heating rate by conventional DSC. The line is a guide to the eye.

EXPERIMENTAL

Materials and Sample Preparation

The epoxy system studied was an epoxy resin based on diglycidyl ether of bisphenol A (DGEBA) (Araldite LY564 from CIBA Speciality Chemicals) and cured with a diamine based on 4,4′-diamino-3,3′-dimethyldicyclohexylmethane (3DCM) (HY 2954 from CIBA Speciality Chemicals). The epoxy equivalent of the resin was 170 g equiv^{-1}. The resin and the amine were mixed in a stoichiometric ratio (weight ratio 100 : 35) at room temperature, stirred for 10 min and then degassed in a vacuum chamber for 10–15 min. Finally, the samples were enclosed in aluminium pans for calorimetric analysis.

Calorimetric Measurements

The temperature modulated DSC measurements were performed with a Mettler-Toledo 821e equipped with an intracooler, and STAR® software was used for alternating DSC (ADSC) evaluation, which is the TMDSC technique commercialised by Mettler-Toledo. In the following sections of this work, we will refer to ADSC to indicate the TMDSC measurements. The temperature and heat-flow calibrations were performed using indium and zinc standards. The modulation conditions used in the quasi-isothermal curing reaction were an amplitude of 0.5 K and a period of 60 s. The nonisothermal ADSC experiments were performed at an underlying heating rate of 1 K min^{-1}, an amplitude of 0.5 K, and a period of 60 s. To calibrate the heat-flow signal, correct the amplitude, and eliminate the cell asymmetry, ADSC requires a blank with an empty pan on the reference side and an empty pan plus a lid on the sample side, at the same conditions as in the sample measurement. For ADSC measurements τ_{lag} was set to 0.

The DSC measurements were performed at the usual heating rates of 10 K min^{-1}, except for multiscan experiments where heating rates between 2.5 and 20 K min^{-1} were used. The sample weight was approximately 8–10 mg. All the calorimetric scans, ADSC and DSC, were performed with a nitrogen gas flow of 50 mL min^{-1}.

Thermogravimetric Analysis

Loss of weight was measured using a Mettler-Toledo TG 50 thermogravimetric analyzer in a temperature range between 40 and 600°C at heating rates between 2.5 and 20 K min^{-1} , and a nitrogen gas flow of 200 mL min^{-1}. The temperature scans were performed in samples of about 6 mg of the unreacted mixtures of epoxy and hardener.

RESULTS AND DISCUSSION

Thermal Properties of the Reacting System

The heat of curing ΔH_r has been determined from the nonisothermal heat-flow curves, performed at different heating rates by conventional DSC. As in other epoxy resins,[31] the value of ΔH_r tends to increase as the heating rate decreases. Figure 1 shows this dependence of ΔH_r on the heating rate for values determined by DSC ($q \geq 2.5$ K min^{-1}). An average value of 440 J g^{-1} was taken as the total heat of curing for the calculation of the degree of conversion by the ratio of the partial heat of curing and this value. The glass transition temperature of the unreacted system, T_{go}, determined at 10 K min^{-1}, is −40.4°C. The effect of heating rates lower than 2.5 K min^{-1} on ΔH_r and T_g are shown in a second part of this work, which

Table I Thermal Degradation of the DGEBA-3DCM Resin at Different Heating Rates (q): Onset Temperature (T_{do}), Extrapolated Onset Temperature ($T_{do,e}$), Inflection Temperature (T_{inf})

q (K min^{-1})	T_{do} (°C)	$T_{do,e}$ (°C)	$T_{d,\inf}$ (°C)
2.5	275	328.8	352.1[a]
5	295	339.8	362.8[a]
10	310	353.4	375.5
15	310	355.3	378.1
20	320	359.0	382.4

[a] This temperature is the average between the values of two TGA curves.

includes the study of the nonisothermal curing by TMDSC.[32]

The thermal stability of the reacting system was determined by thermogravimetric analysis (TGA), submitting the unreacted mixture to different heating rates. The onset temperature of the thermal degradation indicates the limiting temperature of the nonisothermal scans. The determination of this temperature is important because the thermal degradation modifies the properties of the crosslinked resin, in particular, decreasing the final glass transition of the epoxy. The characteristic temperatures of the thermal degradation are indicated in Table I: the onset (T_{do}) temperature is the temperature where the loss weight begins, while the onset extrapolated temperature ($T_{do,e}$) is the temperature determined by the crossing of the two tangents to the TGA curve in the beginning of the degradation. The inflection temperature ($T_{d,\inf}$) indicates the temperature where the degradation rate is at its maximum. This temperature is obtained from the peak of the first derivative of the TGA curve.

The glass transition temperature T_g of the fully cured system is usually determined by DSC after the postcure of the sample.[2] When the sample is cured nonisothermally, the T_g is determined in a second scan obtained immediately after the first scan, which is performed nonisothermally up to a temperature where no exothermal reaction is detected, and then cooled to a temperature about T_g −60°C at a controlled rate. The T_g of the epoxy can be obtained in the second scan at a determined heating rate. When the sample is previously cured isothermally, it must be submitted to a postcure in nonisothermal conditions, and the T_g measured in a final scan.

The glass transition temperature of the DGEBA–3DCM system was determined using DSC and ADSC. The determination by DSC was performed on the second scan at a heating rate of 10 K min^{-1} immediately after the first scan heating up 250°C, and cooling at 20 K min^{-1}. This second scan does not show any residual heat of curing. It is observed that the values of T_g, obtained in this second scan, depend on the heating rate of the first scan. The lower the heating rate, the higher the T_g measured in the second scan, as shown in Figure 2. The values of T_g of this figure, like the others reported in this work, are measured at the temperature on the midpoint of the transition. A value of T_g = 143°C is obtained after the nonisothermal curing at a heating rate of 10 K min^{-1}. The dependence of T_g on the heating rate of the curing has also been observed by Barton et al.[33] in an epoxy cured by a modified imidazole. It seems that a slow scan gives a more complete reaction of the functional groups, and additionally, the time of reaction is longer than in a fast scan. The result is a more effective crosslinking of the network.

Differences in the values of T_g have also been observed in samples cured isothermally for different periods of time, postcured nonisothermally at 10 K min^{-1} to a temperature of about 250–270°C and submitted to a final scan under the same conditions. The maximum value of T_g was 120°C, obtained in the postcure at 10 K min^{-1}, after isothermal curing between 60 and 160°C for different periods of time. The T_g of the final scan at 10 K min^{-1} increases to a value which ranges between 132 and 143°C. In particular, the postcure of a sample cured for 10 min at 160°C gives a T_g of 111°C, with practically no residual heat of curing when heated up to 260°C. However, the T_g

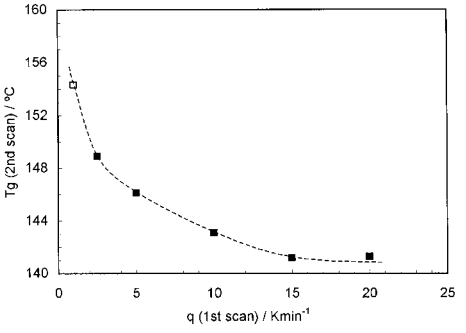

Figure 2 Dependence of the glass transition temperature on the heating rate of the first scan. The T_g was measured in the second scan at 10 Kmin^{-1}. The value at 1 Kmin^{-1} (□) was obtained by the total heat flow signal of ADSC at the same heating rate as the first scan, and the following modulation conditions: 0.5 K of amplitude and 60 s of the period.

of this sample rises to 143°C in the final scan. Similar behavior was also reported by Verchere et al.,[24] and is attributed to the chemical structure of the diamine. The situation of the methyl group in a neighboring position to the amine group yields a steric hindrance that inhibits the reactivity of these groups. The practically complete reaction of the amine groups is achieved after heating at temperatures up to 260°C, giving a resin with a higher T_g. Notwithstanding this special structure of the diamine, the effect of time and temperature of cure on the final T_g has also been observed in other epoxy resins.[33,34]

The glass transition temperature has also been determined by ADSC in samples with the following thermal history: isothermally cured between 40 and 140°C for different periods of time, postcured at an underlying heating rate of 1 K min^{-1} up to 270°C, with modulation conditions of 0.5 K and 60 s, and a final scan under the same conditions. The T_g of the final scan measured on six curves of total heat flow gives an average value of $T_{g,\langle\phi\rangle} = 154.3 \pm 0.8$°C. According to the effect of the previous thermal history, this result agrees with the T_g obtained by conventional DSC, because the underlying heating rate used in ADSC is lower than in DSC.

The glass transition temperature determined by DSC is usually called thermal or conventional glass transition to differentiate it from the dynamic glass transition temperature. The former is heating rate dependent and the latter is frequency dependent. The TMDSC allows us to determine the dynamic glass transition using the real part of the heat capacity, C'_p, which in this transition is practically equal to the modulus of the complex heat capacity $|C^*_p|$. The dynamic glass transition determined on the $|C^*_p|$ signal of the final scan obtained under the same conditions (1 K min^{-1}, 0.5 K, 60 s) is $T_{g,|Cp^*|} = 156.1 \pm 0.9$°C. As shown elsewhere,[28–30] the value of $T_{g,|Cp^*|}$ is slightly higher than the value measured from the total heat flow $T_{g,\langle\phi\rangle}$.

The Vitrification Process

The vitrification of a thermosetting system has been widely studied by the residual heat of curing method.[2] After different periods of curing, the residual heat of curing and the T_g are measured. The former is used to calculate the degree of conversion by the expression

$$\alpha = 1 - \frac{\Delta H_{\text{res}}}{\Delta \text{H}_\text{r}} \tag{10}$$

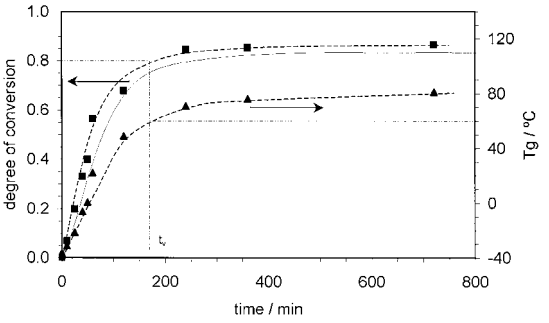

Figure 3 Variation of the degree of conversion (■) and the T_g (▲) for the isothermal curing of the DGEBA-3DCM resin at 60°C. The dashed lines are a guide for the eye. The degree of conversion was determined by the residual heat of curing. The vitrification time is obtained when $T_g = T_c = 60$°C. The solid line gives the conversion calculated from the total heat flow ADSC signal.

where ΔH_{res} and ΔH_r are, respectively, the residual and the total heat of curing. In our epoxy system the value of ΔH_r was taken as 440 J g^{-1}. The values of the degree of conversion and the T_g for a curing temperature of 60°C are shown in Figure 3. The study of the vitrification process by DSC is based on these data: the system vitrifies when the T_g equals the curing temperature. At this temperature, the vitrification time is estimated at 170 min for a degree of conversion of about 0.8. As we will show below, TMDSC gives an alternative way to determine the properties of the system at vitrification.

The total heat flow signal, $\langle\phi\rangle$, measured by ADSC, shows the exothermic peak of the curing reaction, which allows the degree of conversion to be calculated. Other information about the vitrification process is given by the complex heat capacity and the phase angle. These signals are shown in Figure 4 for a curing temperature of 70°C.

The variation of the degree of conversion with time, calculated from the total heat flow, is shown in Figure 5 for different curing temperatures. The comparison of the curves $\alpha - t$ in the DGEBA–3DCM system, at 60°C, shows slight differences. Figure 3 shows the conversion calculated from the $\langle\phi\rangle$ signal (continuous line), which deviates from the values obtained by the residual heat of curing method (dashed line). These differences, whose maximum is about 0.5 units of the degree of conversion, may arise from underestimation of the residual heat of curing that increases the conversion. The determination of the degree of conversion from the total heat flow ADSC curves has the

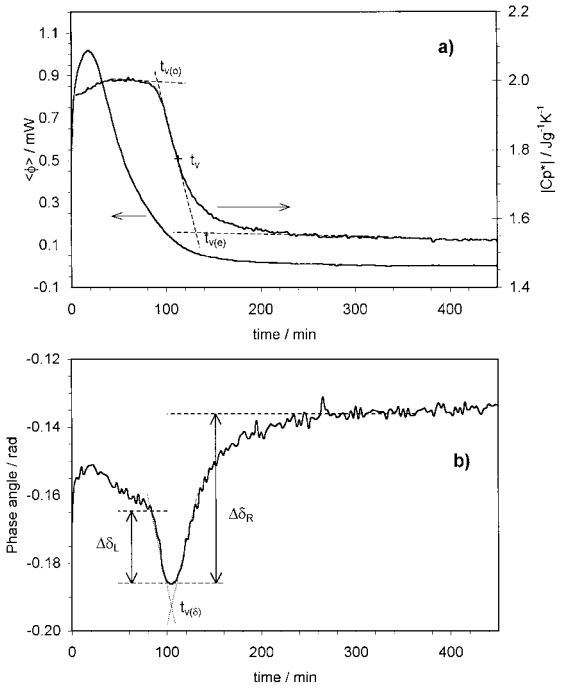

Figure 4 Total heat flow and modulus of C_p^* (a) and phase angle (b) for the curing of the DGEBA-3DCM system at a temperature of 70°C. Modulation conditions: 0.5 K of amplitude and 60 s of the period. The extrapolated onset ($t_{v(o)}$), midpoint (t_v), and endset ($t_{v(e)}$) vitrification times are indicated in the curve of $|C_p^*|$ (a). Similarly, the phase angle curve (b) shows the vitrification time by the extrapolated peak [$t_{v(\delta)}$] and the intensity of the relaxation by the changes $\Delta\delta_R$ and $\Delta\delta_L$.

usual limitations of the heat flux differential scanning calorimeters. In our DGEBA–3DCM resin, at temperatures higher than 100°C the peak of the exothermic reaction takes place during the first minutes of the reaction and an uncontrolled amount of heat is lost. On the other

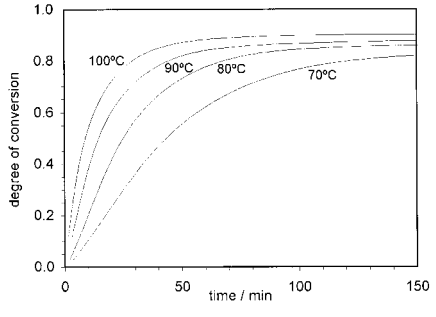

Figure 5 Variation of the degree of conversion with the time of curing for temperatures between 70 and 100°C. The degree of conversion was calculated from the total heat flow ADSC signal.

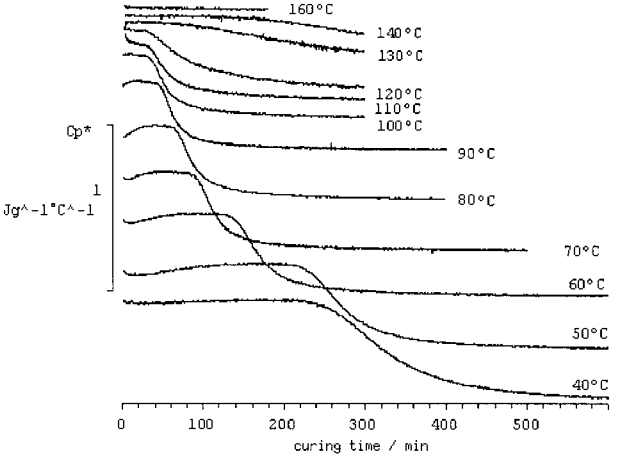

Figure 6 Modulus of C_p^* for the DGEBA-3DCM resin at different curing temperatures. Modulation conditions: 0.5 K of amplitude and 60 s of the period.

hand, at curing temperatures lower than 50°C the heat flow signal is so small that it is difficult to obtain reliable data to calculate the conversion. In addition, the exothermicity at the beginning of the reaction induces a distortion in the modulated heat-flow signal that affects the initial values of the heat capacity and the phase angle.

The modulus of the complex heat capacity, $|C_p^*|$, shows a variation that is similar to that observed in other epoxy–amine systems.[12–14,17,18] As shown in Figure 4, the $|C_p^*|$ tends initially to increase slightly and in this case, levels off, presenting a plateau. This plateau is observed in practically all the isotherms analysed, as shown in Figure 6. The variation of $|C_p^*|$ in this step may be attributed to the growth of the linear chains as the reaction of primary amine groups proceeds.[12,13] Further formation of the network structure as the reaction of the second amine group takes place may give a decrease in $|C_p*|$, as was observed in a diepoxide–polypropylenetriamine system.[18] In the present DGEBA–3DCM resin, $|C_p^*|$ tends to be constant, probably due to the difficulties the secondary amine groups have in reacting. In other model systems such as a diepoxide–methylene dianiline, $|C_p^*|$ continuously increases in this step.[35]

After this step, a decay in $|C_p^*|$ is observed, which is attributed to the vitrification of the system.[12–14,16–23] As the crosslinking progresses, there is a characteristic time where the number of configurational states significantly decrease, and correspondingly, there is a decrease in the heat capacity of the system. In addition, assuming that the average relaxation time of segmental chains

Table II Vitrification Properties Determined by ADSC from the Complex Heat Capacity in the DGEBA-3DCM Resin

T_c(°C)	$t_{v(o)}$[a] (min)	t_v[b] (min)	α_v	$t_{v(e)}$[c] (min)	$t_{v(\delta)}$[d] (min)	α_{lim}
40	247.3	317.7	—	389.6	296	—
50	225.5	269.7	—	312.9	251.6	—
60	136.7	166	0.76	200	156	0.84
70	91.1	111.6	0.78	132	104	0.85
80	65.6	85.5	0.83	104.1	78	0.87
90	46.5	62.7	0.85	79.2	56	0.88
100	34.4	54.1	0.88	69.7	45	0.90
110	34	53.6	—	72.2	46	—
120	34	77.8	—	105	≈50	—
130	77	≈160	—	≈237	≈130	—

T_c is the curing temperature. The values of the conversion at t_v (α_v) and the limiting conversion (α_{lim}) are only available in the interval of curing temperatures between 60 and 100°C.

[a] Time corresponding to the extrapolated onset of the vitrification.

[b] Time corresponding to the midpoint of the vitrification.

[c] Time corresponding to the extrapolated endset of the vitrification.

[d] Time of the vitrification measured by the peak of the phase angle.

in the glassy state is between 50 and 100 s,[36] and taking into account that the time scale of ADSC measurements is 60 s, it turns out that the relaxation process detected by ADSC, via the abrupt decay on $|C_p^*|$, corresponds to the macroscopic vitrification of the system. Therefore, the reaction becomes practically frozen in, and the diffusion of the reacting groups controls the kinetics.

This change of $|C_p^*|$ is similar to the sigmoidal shape of the vitrification shown by cooling through the glass transition region.[27,30,37] The system undergoes a structural relaxation, going from a rubber-like state, corresponding to the highest value of $|C_p^*|$, to another state that is typical of a glass at the lowest value of $|C_p^*|$. The difference with the glass transition is that the composition of the system changes slightly, as a consequence of small changes due to the diffusion of the reactive groups. However, the degree of conversion tends to a practically constant limiting value, as shown in Figure 5, for different curing temperatures. The values of the limiting degree of conversion, α_{lim}, are indicated in Table II.

The interval of vitrification of the system is well determined by the onset time ($t_{v(o)}$) and the endset time ($t_{v(e)}$). A vitrification time (t_v) may be defined as the time at the midpoint of $\Delta|C_p^*|$, namely

$$\Delta|C_p^*| = |C_p^*|(t_{v(o)}) - |C_p^*|(t_{v(e)}) \qquad (11)$$

where $|C_p^*|(t_{v(o)})$ and $|C_p^*|(t_{v(e)})$ are the values of $|C_p^*|$ at the extrapolated onset and endset points. The definition of the endset time has an operational meaning to allow the determination of $\Delta|C_p^*|$ or the time interval of the vitrification. The change of $|C_p^*|$ in the vitrification tends to decrease as the curing temperature increases, as shown in Figure 7. The value of $\Delta|C_p^*|$ should be zero when the temperature is equal to the maximum T_g of the system. This effect has also been observed in other epoxy resins.[18,21]

The vitrification time determined by the $|C_p^*|$ signal agrees very well with the value determined by the residual heat of curing method. In our DGEBA–3DCM resin, t_v at a curing temperature of 60°C is 166 min and, as mentioned above, the vitrification time estimated by the residual heat of curing method (Fig. 3) is about 170 min. The properties of the vitrification interval are summarized in Table II.

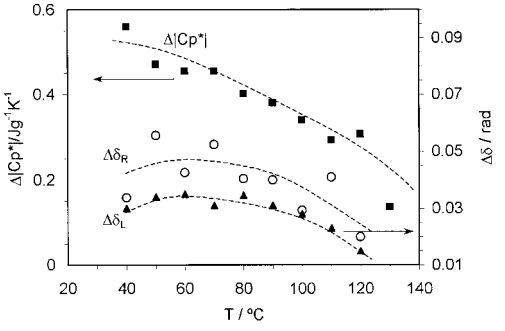

Figure 7 Dependence of the variation of $|C_p^*|$ (■) and the height of the phase angle, $\Delta\delta_R$ (○) and $\Delta\delta_L$ (▲). The dashed lines are a guide to the eye for the variation of $\Delta|C_p^*|$, $\Delta\delta_R$ and $\Delta\delta_L$.

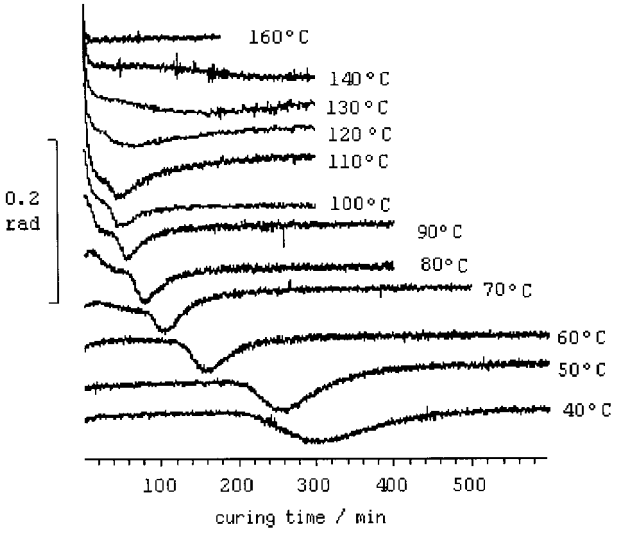

Figure 8 Uncorrected phase angle for the DGEBA-3DCM resin at different curing temperatures. Modulation conditions: 0.5 K of amplitude and 60 s of the period.

Alternatively, the vitrification may be detected by measuring the phase angle (δ) between the heat flow and the heating rate. Figure 8 shows the uncorrected phase angle measurements for different curing temperatures. The relaxation associated to the vitrification process shows an asymmetric peak of the phase angle signal, which is sharper at the beginning of the relaxation than at the end, where the change is more gradual. At curing temperatures higher than 70°C, a peak in the opposite direction from the peak of vitrification is observed. This peak is attributed to the high exothermicity of the system because it corresponds to the maximum heat flow evolved during the reaction. At temperatures higher than 110°C this peak becomes wider as a consequence of the larger extension of the interval of vitrification.

The measurement of the time of this peak $t_{v(\delta)}$, which is shown in Figure 4(b), also gives the vitrification time. Table II shows the time of the extrapolated peak of the phase angle, which agrees well with the vitrification time t_v measured from $|C_p^*|$, notwithstanding an advance of the former with respect to the latter.

The intensity of this peak may be measured by the height between the maximum value and the right side of the peak, $\Delta\delta_R$, or alternatively between the maximum value and the left side, $\Delta\delta_L$. Both properties are defined in Figure 4(b), and the dependence of these values on the curing temperature is shown in Figure 7, together with the so-called intensity of the vitrification measured by $\Delta|C_p^*|$. The behavior of the intensity of the phase angle peak is slightly different from that of $\Delta|C_p^*|$. Although $\Delta|C_p^*|$ decreases quasi-linearly with T_c, both values, $\Delta\delta_R$ and $\Delta\delta_L$, tend to increase at low T_c and finally also decrease.

As mentioned earlier, in addition to the effects of the thermal relaxation and the chemical reaction, the phase angle depends on the frequency, the change of the heat capacity experimented in the relaxation, and the thermal conductance between the sample-pan and the measuring thermocouple.[20,28–30] All of these parameters should be taken into account to correct the phase angle peak and obtain the value which corresponds to the vitrification. The methodology to perform the correction of the phase angle during the curing reaction has been recently shown by Schawe.[20] Therefore, the results of the uncorrected phase angle shown in Table II on the vitrification, and those of Figures 7 and 8, have a semi-quantitative value.

Time–Temperature–Transformation Cure Diagram

The values of the midpoint vitrification time may be used to build the vitrification line in the TTT cure diagram as shown by the filled squares in Figure 9. In addition, the onset (◆) and the endset (▲) of the vitrification, which determine the interval of vitrification, are also shown in Figure 9. The diagram shows a part of the usual sigmoidal shape shown in other epoxy–diamine resins.[5,7] In the lower temperature part, the TTT diagram usually has a maximum of the vitrification time,

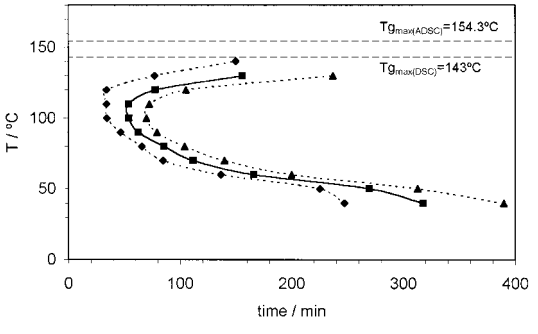

Figure 9 Time–temperature–transformation diagram showing the vitrification interval determined from the $|C_p^*|$ signal: onset vitrification time (◆), midpoint vitrification time (■), and endset vitrification time (▲). The continuous and dotted lines are a guide for the eye. The maximum T_g obtained by DSC ($T_{g\max(\mathrm{DSC})}$ = 143°C) and ADSC ($T_{g\max(\mathrm{ADSC})}$ = 154.3°C) are shown by dashed lines (see the text for additional details on these measurements).

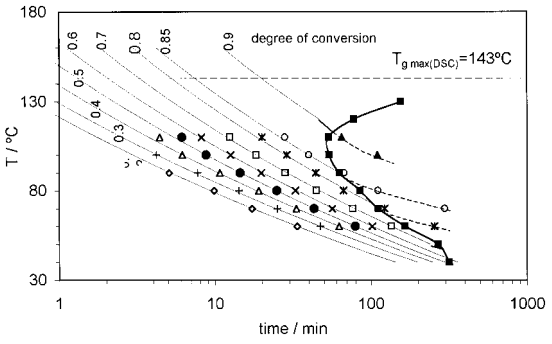

Figure 10 Time–temperature–transformation diagram showing the vitrification times (■) and the iso-conversion lines (continuous lines), which were calculated by eq. (16). The extrapolation of the iso-conversion line within the glassy state (dotted line) for α = 0.8, 0.85, and 0.9 is a guide for the eye. The symbols on the iso-conversion lines are experimental values obtained by the conversion–time data.

which then decreases as the temperature approaches the T_{go} of the unreacted system. This maximum is not observed in the TTT diagram of Figure 9, because the lowest temperature of curing was 40°C, but at this temperature a slight change in the slope of the vitrification line is detected. Between 40 and 100°C the vitrification time tends to decrease with the curing temperature to a minimum value at about 100–110°C, and at higher temperatures t_v increases with T_c. The minimum of t_v is a consequence of the opposing effects of the increasing of the constant of the reaction rate and the decreasing of the reactants at vitrification as the maximum T_g is approached.[7]

However, it seems difficult to complete the vitrification line up to the temperature of the maximum glass transition, which is 154.3°C, in this DGEBA–3DCM system. As mentioned above, due to the steric hindrance of the amine groups, it is not possible to achieve this maximum temperature by isothermal curing. This value of T_g was obtained by ADSC in nonisothermal curing at a heating rate of 1 K min^{-1}. Nevertheless, the vitrification line tends to a limiting value of 140°C, which is close to the maximum T_g obtained by DSC ($T_{g\max\ (DSC)}$ = 143°C) after an isothermal curing period of time.

The TTT diagram may be completed by the iso-conversion lines, as shown in Figure 10. The building of these lines is performed from the time–temperature shift of the degree of conversion against the curing time. The kinetic analysis of the chemical reaction of curing is based on the following fundamental equation:

$$\frac{d\alpha}{dt} = k(T)f(\alpha) \tag{12}$$

where $k(T)$ is the reaction rate constant and $f(\alpha)$ is a function of the conversion degree. Rearranging and integrating eq. (12), the following equation is obtained:

$$g(\alpha) = \int_o^\alpha \frac{d\alpha}{dt} = k(T)t \tag{13}$$

where $g(\alpha)$ is dependent only on the degree of conversion. Taking logarithms and assuming an Arrhenius form of $k(T) = A\exp(-E_a/RT)$, where A is the preexponential factor and E_a the apparent activation energy, produces the following form of eq. (13):

$$F(\alpha) = \ln g(\alpha) = \ln A - (E_a/RT) + \ln t \tag{14}$$

where $F(\alpha)$, which is also a function only of the conversion degree, describes the variation of the degree of conversion with the time and the curing temperature.

The apparent activation energy may be calculated at different degrees of conversion by eq. (14). The slope of the plot of ln t against T^{-1}, at a fixed degree of conversion, gives E_a:

$$\frac{E_a}{R} = \frac{d\ln t}{d(1/T)} \tag{15}$$

In the present work, the calculation of E_a was performed from the results of the degree of conversion for the isotherms obtained by ADSC from 60 to 100°C, using only the values of α at times below the onset of vitrification. The values of E_a from degrees of conversion between 0.2 and 0.7 are shown in Table III. For the indicated interval of temperatures, the vitrification takes place at degrees of conversion higher than 0.7, and eq. (14) may not be applied.

From the values of E_a at different conversions, an average value of 57.9 ± 4.4 kJ mol^{-1} was calculated. This value is in good agreement with that calculated by the Kissinger method of 58.7 kJ mol^{-1}, from the peak temperature of DSC scans obtained at heating rates between 2.5 and 20 K min^{-1}. Both values of E_a also agree with that estimated by Verchère et al.,[24] namely between 56 and 59 kJ mol^{-1}.

Table III Apparent Activation Energy Calculated by the Isoconversional Method Using the Total Heat Flow Data of Isothermal ADSC Scans

Degree of Conversion	E_a (kJ mol^{-1})
0.2	62.7
0.3	62.2
0.4	59.7
0.5	56.9
0.6	54.2
0.7	51.7
Average value	57.9 ± 4.4

By the value of E_a at each degree of conversion one can build the iso-conversion lines by the application of eq. (14), slightly reordered:

$$\ln t_2 = \ln t_1 + \frac{E_a}{R}\left(\frac{1}{T_2} - \frac{1}{T_1}\right) \tag{16}$$

where t_1 is the time of curing at the temperature T_1, for a fixed conversion, determined on the $\alpha - t$ curves, and t_2 is the calculated time of curing at the temperature T_2. Figure 10 shows the iso-conversion lines in the TTT cure diagram of the DGEBA–3DCM system. The lines at α 0.8, 0.85, and 0.9 were obtained by using the same E_a value as for $\alpha = 0.7$. The symbols on the iso-conversion lines are the experimental values derived from the $\alpha - t$ curves. Obviously, at times higher than t_v there is a deviation between the experimental values and the iso-conversion lines, because the kinetics is diffusion controlled. It must be noted that the use of a constant value of E_a (e.g., the average value of $E_a = 57.9$ kJ mol^{-1}) gives significant deviations from the experimental points (not shown in this work).

The gelification of this DGEBA–3DCM system was studied by Verchère et al.[24] using the method of solubility in tetrahydrofurane. A value of conversion close to 0.6 was determined. Taking this value into account, the gel T_g determined at the crossing point between the line $\alpha = 0.6$ and the onset of vitrification is about 46°C. This value agrees with that of slightly above 50°C, reported by the same authors.[24]

Kinetic Analysis of the Diffusion-Controlled Regime

As mentioned before, the kinetics of the curing reaction changes from control by the chemical reactivity of the functional groups, whose reaction rate is governed by eq. (12), to a controlled diffusion kinetics. One method for analyzing the reaction in this regime uses the model of Rabinowitch,[38] which introduces an overall effective rate constant $k_e(T,\alpha)$. This constant may be calculated from the rate constant of the chemical reaction, $k(T)$, which is the same as in eq. (12), and the rate constant of the diffusion controlled step, $k_{\text{diff}}(T,\alpha)$:

$$\frac{1}{k_c(T,\alpha)} = \frac{1}{k(T)} + \frac{1}{k_{\text{diff}}(T,\alpha)} \tag{17}$$

The diffusion rate constant may be modeled in terms of a Williams–Landel–Ferry type equation,[5,19,39] the Adam-Gibbs theory,[40] or conditioning the diffusion control to a critical value of the conversion.[41] According to this last approach, a diffusion factor $DF(T,\alpha)$ may be defined as the ratio of the constants $k_e(T,\alpha)/k(T)$, and alternatively $DF(T,\alpha)$ may be obtained by dividing the experimental values of the reaction rate by those predicted by a chemical kinetic model:

$$DF(T,\alpha) = \frac{\left(\frac{d\alpha}{dt}\right)_{\text{exp}}}{\left(\frac{d\alpha}{dt}\right)_{\text{chem}}} \tag{18}$$

The chemical rate $(d\alpha/dt)_{\text{chem}}$ may be calculated by eq. (12), previously defining a function of $f(\alpha)$. As in other epoxy resins,[31,42] we use the simplified autocatalytic model (Sesták-Berggren model)

$$f(\alpha) = \alpha^m(1 - \alpha)^n \tag{19}$$

The kinetic parameters were calculated by the method proposed by Málek[43] with $E_a = 58$ kJ mol^{-1}. The analysis of the isotherm at 70°C gives the following set of kinetic parameters: ln $A = 13.06$, $m = 0.47$, and $n = 1.76$. These values reproduce the experimental values of the reaction rate between $\alpha = 0.2$ and $\alpha = 0.7$ very well, as shown in Figure 11, where the reaction rate is plotted against the degree of conversion. For values of $\alpha \leq 0.2$, a deviation between the experimental (continuous line) and the chemical kinetic values (dotted line) is observed because $f(\alpha)$ tends to zero when the degree of conversion tends also to zero, and the experimental value of the reaction rate is not zero at the beginning of the reaction. Nevertheless, this deviation does not affect the vitrification region, which appears at a degree of conversion of about 0.75. Other equations, such

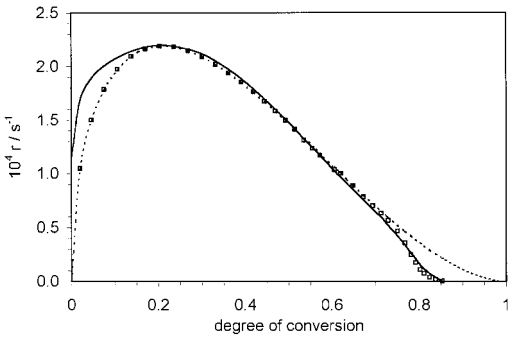

Figure 11 Variation of the reaction rate ($r = d\alpha/dt$) against the degree of conversion, for the curing of the DGEBA-3DCM at 70°C. The continuous line corresponds to the experimental values, the dotted line to the chemical kinetic values calculated by the Sesták-Berggren model, without mobility restrictions, and the open squares to the simulated rate obtained by the product of the chemical kinetic values and the mobility factor.

as that for the autocatalytic behaviour proposed by Kamal,[44] could give a better fit in this low conversion region. The study in other epoxy resins with other kinetic models is currently in progress. The other deviation at a conversion of about 0.7 is due to the vitrification of the system. The diffusion factor $DF(T,\alpha)$ may be now calculated by eq. (18). The values of DF in the conversion interval between 0.4 and 0.9 are shown in Figure 12 by the dotted line.

As proposed by Van Mele et al.,[13,14] the measurements of the heat capacity in curing reactions by TMDSC give a mobility factor $MF(T,\alpha)$ that in many systems may be identified with the diffusion factor defined above. The mobility factor is defined by the following expression:

$$MF(\alpha,T) = \frac{|C_p^*|(t,T) - |C_{p,g}^*|(T)}{|C_{p,l}^*|(t,T) - |C_{p,g}^*|(T)} \qquad (20)$$

where $|C_p^*|\,(t,T)$ is the actual value of $|C_p^*|$, $|C_{p,g}^*|(T)$ is the value of $|C_p^*|$ in the glassy state assigned to the long curing time, and $|C_{p,l}^*|(t,T)$ is the $|C_p^*|$ in the liquid state, before the vitrification of the system. During the vitrification, the value of $|C_{p,l}^*|(t,T)$ is obtained by the linear extrapolation of $|C_p^*|$ in the liquid state. However, in our DGEBA–3DCM, this extrapolation is not necessary because the values of $|C_p^*|$ in the liquid state before vitrification are practically constants. The mobility factor at 70°C is also shown in Figure 12 by the continuous line. The good agreement between $MF(T,\alpha)$ and $DF(T,\alpha)$ in this DGEBA–3DCM system allows us to obtain a simulated reaction rate from the chemical reaction rate corrected by the mobility factor:

$$\left(\frac{d\alpha}{dt}\right)_{\text{sim}} = \left(\frac{d\alpha}{dt}\right)_{\text{chem}} \cdot MF(T,\alpha) \qquad (21)$$

The values of the simulated reaction rate, which are shown by open squares in Figure 11, are in very good agreement with the experimental reaction rate (continuous line). These results show that TMDSC gives a method for determining the time and composition corresponding to the start of the reaction controlled by diffusion and for studying the overall kinetics analysis. Other results in epoxy resins show the validity of the method.[13,14,18] Nevertheless, in other curing reactions some differences between $MF(T,\alpha)$ and $DF(T,\alpha)$ may be found.[13,45]

CONCLUSIONS

The isothermal cure of an epoxy resin based on diglycidyl ether of bisphenol A (DGEBA) with a diamine based on 4,4′-diamino-3,3′-dimethyldicyclohexylmethane (3DCM) was analyzed by conventional DSC and ADSC, which is a TMDSC technique. The calorimetric data show that the heat evolved during the curing increases when the heating rate decreases. According to other authors,[33] this dependence is due to the effect of topological constraints in the highly crosslinked network. These constraints are reduced when the heating rate is slower, producing an increase in the heat of curing. The analysis of the thermal degradation gives the limiting temperature of the

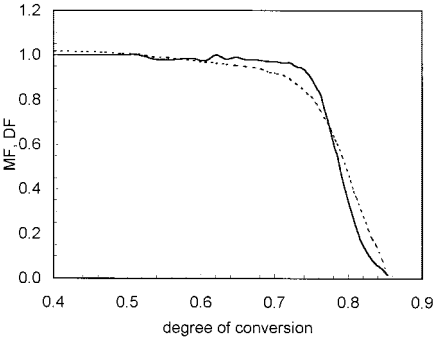

Figure 12 Variation of the mobility factor MF(T,α) obtained from the C_p^* signal (continuous line), and the diffusion factor DF(T,α), obtained from the ratio of experimental and chemical reaction rates (dashed line).

nonisothermal DSC and ADSC scans to avoid the rupture of crosslinks and the corresponding decrease of the final T_g.

The measurement of the glass transition temperature of samples submitted to postcure shows that the heating rate of cure and the postcure conditions have a considerable effect on the final properties of the network. The effect of the heating rate of cure on T_g has the same nature as that on the heat of curing. The slower the heating rate, the more complete crosslinking reaction is obtained and, additionally, the reaction time is longer. Both effects give an increase in the T_g. Apart from these effects, the situation of the methyl groups in the 3DCM in a neighboring position to the amine group yields a steric hindrance that inhibits the full reaction, even at 160°C. All these aspects show the difficulty to achieve the so-called "fully cured" epoxy, which indicates a resin with a degree of conversion of one. The $T_{g\infty}$ of the "fully cured" epoxy is defined as the maximum value of T_g of the resin. In our DGEBA–3DCM resin, the maximum glass transition ranges between 143 and 154°C, depending on the previous thermal treatment and the technique, DSC, or ADSC, respectively.

ADSC simultaneously gives information on the evolution of the total heat flow, which allows us to calculate the degree of conversion, and also the complex heat capacity, which gives a direct method of studying the vitrification of the resin. From the vitrification time, the corresponding vitrification line may be determined and used to build the TTT cure diagram of the resin. More information about the intensity of the vitrification may be found from the variation of the complex heat capacity. The phase angle is also sensitive to the relaxation associated with the vitrification, but this property is subjected to some corrections.

The chemical kinetics has been studied by a simplified autocatalytic model [$f(\alpha) = \alpha^m(1 - \alpha)^n$, Sesták-Berggren model] with an apparent activation energy of 58 kJ mol^{-1}. The diffusion factor, which is obtained from the ratio of the experimental and chemical reaction rates, is practically equal to the mobility factor determined by the variation of the $|C_p^*|$ signal during the vitrification interval. This equality allows the analysis of the step where the mobility of the functional groups is extremely low and the kinetics is controlled by their diffusion. In this case, the simulation of the overall reaction rate obtained by the product of the chemical reaction rate and the mobility factor agrees very well with the experimental reaction rate.

Financial support has been provided by CICYT (MAT97-0634-C02-02). The authors are grateful to CIBA Speciality Chemicals for supplying the epoxy and the hardener.

REFERENCES

1. Fava, R. A. Polymer 1968, 9, 137.
2. Prime, B. In Thermal Characterization of Polymeric Materials; Turi, E. A., Ed.; Academic Press: San Diego, 1997, vol. 2, Chap. 6.
3. Barton, J. M. In Epoxy Resins and Composites I; Dusek, K., Ed.; Advances in Polymer Science; Springer-Verlag: Berlin, 1985, p. 112, vol. 72.
4. Ellis, B. In Chemistry and Technology of Epoxy Resins; Ellis, B., Ed.; Chapman and Hall: Glasgow, 1996, Chap. 6.
5. Wisanrakkit, G.; Gillham, J. K. J Coatings Technol 1990, 62, 35.
6. Prime, R. B. J Therm Anal 1986, 31 1091.
7. Enns, J. B.; Gillham, J. K. J Appl Polym Sci 1983, 28, 2567.
8. Gillham, J. K. Polym Int 1997, 44, 262.
9. Williams, R. J. J. In Polymer Networks, Principles of their Formation, Structure and Properties; Stepto, R. F. T., Ed.; Chapman and Hall: London, 1998, Chap. 4.
10. Reading, M. Trends Polym Sci 1993, 1, 248.
11. Reading, M.; Elliot, D.; Hill, V. L. J Therm Anal 1993, 40, 949.
12. Cassettari, M.; Salvetti, G.; Tombari, E.; Veronesi, S.; Johari, G. P. J Polym Sci Polym Phys 1993, 31, 199.
13. Van Assche, G.; Van Hemelrijck, A.; Rahier, H.; Van Mele, B. Thermochim Acta 1995, 268, 121.
14. Van Assche, G.; Van Hemelrijck, A.; Rahier, H.; Van Mele, B. Thermochim Acta 1997, 304/305, 317.
15. Van Hemelrijck, A.; Van Mele, B. J Therm Anal 1997, 49, 437.
16. Tatsumiya, S.; Yokokawa, K.; Miki, K. J Therm Anal 1997, 49, 123.
17. Swier, S.; Van Assche, G.; Van Hemelrijck, A.; Rahier, H.; Verdonck, E.; Van Mele, B. J Therm Anal 1998, 54, 585.
18. Montserrat, S.; Cima, I. Thermochim Acta 1999, 330, 189.
19. Flammersheim, H. J.; Opfermann, J. Thermochim Acta 1999, 337, 141.
20. Schawe, J. E. K. Thermochim Acta 2000, 361, 97.
21. Lange, J.; Altmann, N.; Kelly, C. T.; Halley, P. J. Polymer 2000, 41, 5949.
22. Van Assche, G.; Verdonck, E.; Van Mele, B. Polymer 2001, 42, 2959.
23. Montserrat, S.; Roman, F.; Colomer, P. J Polym Sci Polym Phys, submitted.
24. Verchère, D.; Sautereau, H.; Pascault, J. P.; Riccardi, C. C.; Moschiar, S. M.; Williams, R. J. J. Macromolecules 1990, 23, 725.

25. Prigogine, I. Introduction to Thermodynamics of Irreversible Processes; Wiley: New York, 1967.
26. Schawe, J. E. K.; Höhne, G. W. H. Thermochim Acta 1996, 287, 213.
27. Schawe, J. E. K. Thermochim Acta 1995, 261, 183.
28. Weyer, S.; Hensel, A.; Schick, C. Thermochim Acta 1997, 304/305, 267.
29. Jiang, Z.; Imrie, C. T.; Hutchinson, J. M. Thermochim Acta 1998, 315, 1.
30. Montserrat, S. J Therm Anal Cal 2000, 59, 289.
31. Montserrat, S.; Andreu, G.; Cortés, P.; Calventus, Y.; Colomer, P.; Hutchinson, J. M.; Málek, J. J Appl Polym Sci 1996, 61, 1663.
32. Montserrat, S.; Martín, J. G. Thermochim Acta, in press.
33. Barton, J. M.; Hamerton, I.; Howlin, B. J.; Jones, J. R.; Liu, S. Polymer 1998, 39, 1929.
34. Montserrat, S. J Therm Anal 1993, 40, 553.
35. Montserrat, S. unpublished results.
36. Kovacs, A. J.; Aklonis, J. J.; Hutchinson, J. M.; Ramos, A. R. J Polym Sci Polym Phys 1979, 17, 1097.
37. Hutchinson, J. M. Thermochim Acta 1998, 324, 165.
38. Rabinowitch, E. Trans Faraday Soc 1937, 33, 1225.
39. Wise, C. W.; Cook, W. D.; Goodwin, A. A. Polymer 1997, 38, 3251.
40. Havlícek, I.; Dusek, K. In Crosslinked Epoxies; Sedlácek, B.; Kahovec, J., Ed.; Walter de Gruyter: Berlin, 1987, p. 417.
41. Cole, K. C.; Hechler, J. J.; Noël, D. Macromolecules 1991, 24, 3098.
42. Montserrat, S.; Málek, J. Thermochim Acta 1993, 228, 47.
43. Málek, J. Thermochim Acta 1992, 200, 257.
44. Kamal, M. R. Polym Eng Sci 1974, 14, 231.
45. Montserrat, S.; Pla, X. Thermochim Acta, submitted.